



# Acceptance Testing and Commissioning of Robotic Intensity-Modulated Radiation Therapy M6 System Equipped with InCise™2 Multileaf Collimator

Jeongmin Yoon\*, Kwangwoo Park<sup>†</sup>, Jin Sung Kim<sup>†</sup>, Yong Bae Kim<sup>†</sup>, Ho Lee<sup>†</sup>

\*Department of Radiation Oncology, Seoul National University Hospital, <sup>†</sup>Department of Radiation Oncology, Yonsei University College of Medicine, Seoul, Korea

**Received** 24 March 2018

**Revised** 26 March 2018

**Accepted** 26 March 2018

**Corresponding author**

Ho Lee

(holee@yuhs.ac)

Tel: 82-2-2228-4363

Fax: 82-2-2227-7823

This work reports the acceptance testing and commissioning experience of the Robotic Intensity-Modulated Radiation Therapy (IMRT) M6 system with a newly released InCise™2 Multileaf Collimator (MLC) installed at the Yonsei Cancer Center. Acceptance testing included a mechanical interdigitation test, leaf positional accuracy, leakage check, and End-to-End (E2E) tests. Beam data measurements included tissue-phantom ratios (TPRs), off-center ratios (OCRs), output factors collected at 11 field sizes (the smallest field size was 7.6 mm×7.7 mm and largest field size was 115.0 mm×100.1 mm at 800 mm source-to-axis distance), and open beam profiles. The beam model was verified by checking patient-specific quality assurance (QA) in four fiducial-inserted phantoms, using 10 intracranial and extracranial patient plans. All measurements for acceptance testing satisfied manufacturing specifications. Mean leaf position offsets using the Garden Fence test were found to be 0.01±0.06 mm and 0.07±0.05 mm for X1 and X2 leaf banks, respectively. Maximum and average leaf leakages were 0.20% and 0.18%, respectively. E2E tests for five tracking modes showed 0.26 mm (6D Skull), 0.3 mm (Fiducial), 0.26 mm (Xsight Spine), 0.62 mm (Xsight Lung), and 0.6 mm (Synchrony). TPRs, OCRs, output factors, and open beams measured under various conditions agreed with composite data provided from the manufacturer to within 2%. Patient-specific QA results were evaluated in two ways. Point dose measurements with an ion chamber were all within the 5% absolute-dose agreement, and relative-dose measurements using an array ion chamber detector all satisfied the 3%/3 mm gamma criterion for more than 90% of the measurement points. The Robotic IMRT M6 system equipped with the InCise™2 MLC was proven to be accurate and reliable.

**Keywords:** Robotic IMRT, InCise™2 MLC, Commissioning

## Introduction

A Robotic Intensity-Modulated Radiation Therapy (IMRT) M6 system<sup>1,2)</sup> (Accuray, Sunnyvale, CA) with a newly released InCise™2 Collimator (MLC)<sup>3)</sup> was installed at the Yonsei Cancer Center in May 2017. The InCise™2 MLC consists of 52 leaves projecting a width of 3.85 mm at

a plane located at 800 mm source-to-axis distance (SAD). Flattening filter-free photon beam of 6 MV energy can be delivered with the nominal dose rate of 1,000 monitor units (MU)/min. The largest field size projected at 800 mm SAD is 115 mm×100.1 mm and the smallest MLC opening is limited to 7.6 mm×7.7 mm. By utilizing tungsten leaves of thickness 90 mm, the transmission through the InCise™2

MLC leaves is achieved as less than 0.5% relative to 100 mm×100 mm field size at 800 mm SAD. Leaf positioning accuracy is better than 0.95 mm at 800 mm SAD from either direction at all possible orientations, leading to submillimeter accuracy of beam delivery. Besides, internal optical camera provides live images used during treatment to verify that MLC leaves are at the required position before the beam is turned on to deliver dose. Penumbra is better than 3.5 mm in X and Y for 10 mm×10 mm field size and 12 mm in X and 20 mm in Y for 100 mm ×100 mm field size.

The purpose of this paper is to present our acceptance testing and commissioning experiences of Robotic IMRT M6 system with InCise™2 MLC. Acceptance testing included mechanical interdigitation test, leaf positional accuracy, leakage check, and End-to-End (E2E) tests.<sup>4)</sup> Beam data measurements included tissue-phantom ratios (TPRs), off-center ratios (OCRs), and output factors (OFs) collected at 11 field sizes (the smallest field size was 7.6 mm×7.7 mm and largest field size was 115.0 mm×100.1 mm at 800 mm SAD) as well as open beam profiles (0°, 45°, 90°, 135°, 180°, 225°, 270°, 315°).

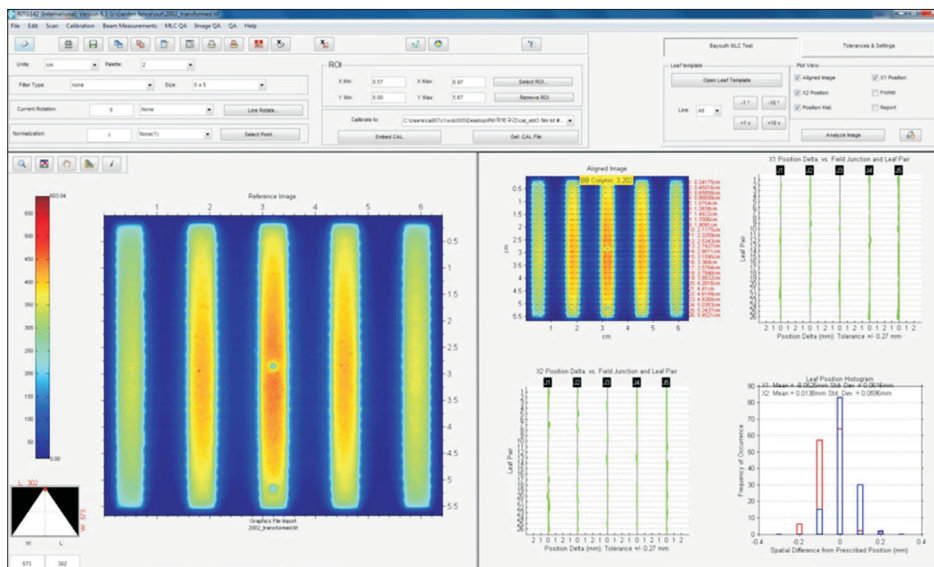


**Fig. 1.** Analysis of leaf positioning accuracy using RIT software.

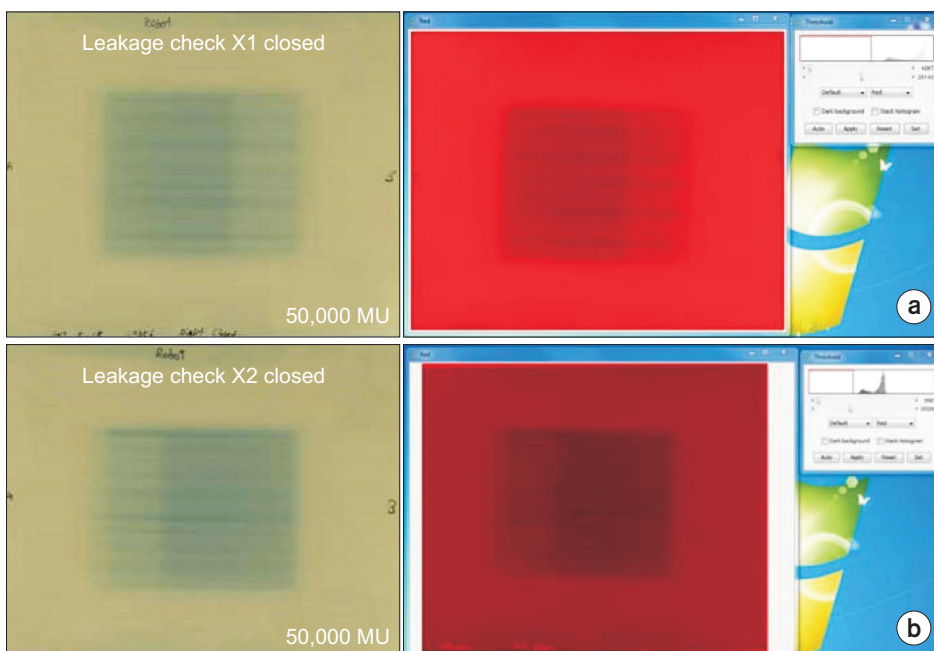


**Fig. 2.** Results of leakage test: (a) EBT3 film and image analysis of X1 closed leakage and (b) EBT3 film and image analysis of X2 closed leakage.

90°, 135° directions). The measurements were compared with the composite data set of countrywide average values. The beam model created with these data was verified by checking patient-specific quality assurance (QA) in fiducial-inserted phantoms.

## Materials and Methods

### 1. Acceptance test

#### 1) Mechanical interdigitation test

This test exercises the ability of the leaves to run a full cycle through the field without colliding with one another. By monitoring the movement of the leaves, we checked if no interlocks are tripped during the movements.

#### 2) Leaf position accuracy

To establish that position accuracy of the InCise™2 leaves, we used the light weight film holder (LWFH) and EBT3 films. The orientation is consistent with garden fence and calibration film. The LWFH build up can only be attached one way due to the guide pins. We delivered picket fence exposure sequence, under geometry parameters with strips to 10 mm, gap to 15 mm, and 170 MU per strip. The films were analyzed using RIT software.

#### 3) Leaf leakage

The purpose of this test is to check that interleaf leakage

is within tolerance. We measured if the maximum leakage in each closed position is less than 0.5% as measured in a ROI of approximately 1 mm<sup>2</sup>.

#### 4) End-to-End (E2E)

This test aims to utilize all components within the system to deliver an accurate treatment plan utilizing the InCise 2 Multileaf Collimator, from CT importation, through planning and delivery. We repeated this test for five tracking modes. For 6D Skull tracking, fiducial tracking, and Xsight Spine tracking modes, an anthropomorphic phantom with a film cube was used. Xsight Lung tracking<sup>5)</sup> used a special phantom platform with Synchrony system. For synchrony respiratory tracking, the film cube should have fiducials embedded in it.

### 2. Beam data collection

All beam data were acquired using a computer-controlled measuring system (MP3-L Therapy Beam Analyzer: PTW, Freiburg, Germany), a Unidos electrometer (PTW), and a PTW 60018 diode SRS (additionally, PTW 60019 microDiamond for OF). Finite size pencil beam (FSPB) dose calculation algorithm requires four measurement data (TPR, OCR, OF, and open beam profiles).

#### 1) Tissue-phantom ratio (TPR)

Central axis TPRs were measured for 11 different fields at

**Table 1.** Percent differences of TPRs between measurement and composite data.

Depth (mm)	7.6× 7.7 (%)	15.4× 15.4 (%)	23.0× 23.1 (%)	30.8× 30.8 (%)	38.4× 38.5 (%)	46.2× 46.2 (%)	53.8× 53.9 (%)	69.2× 69.3 (%)	84.6× 84.7 (%)	100× 100.1 (%)	115× 100.1 (%)
0	-4.05	1.08	0.33	-6.30	-6.16	2.52	-3.46	-5.32	-5.35	-5.27	-5.46
5	-4.81	-7.26	-6.23	-5.44	-5.29	-3.26	-3.84	-3.52	-3.81	-3.07	-3.14
10	-0.80	-1.94	-1.59	-1.87	-1.77	-1.14	-1.27	-1.16	-1.23	-1.16	-1.05
13	-0.08	-0.45	-0.45	-0.65	-0.58	-0.21	-0.33	-0.04	-0.15	-0.09	-0.15
15	0	0	0	0	0	0	0	0	0	0	0
20	0.33	0.37	0.27	-0.11	0.13	0.29	0.21	0.18	0.33	0.33	0.13
30	0.23	0.37	0.33	0.05	-0.02	0.23	0.18	0.23	0.20	0.29	0.25
50	0.83	0.91	0.94	0.81	0.56	0.59	0.46	0.60	0.57	0.64	0.60
100	0.87	1.18	0.81	0.76	0.62	0.86	0.70	0.72	0.87	0.71	0.75
150	1.06	1.07	1.14	0.76	0.78	0.89	1.03	0.77	0.81	0.74	0.77
200	0.81	1.59	1.49	1.31	0.94	0.92	0.98	0.95	0.98	0.91	1.03
250	1.02	1.26	1.45	0.98	0.80	1.30	1.19	1.02	0.99	1.01	1.11
300	0.91	1.41	1.60	1.36	1.04	1.27	1.26	1.31	1.48	1.22	1.32

depths ranging from 0 mm to 300 mm. The reference depth used for normalization of the TPR data was 15 mm for all fields, which is the nominal depth of maximum dose. All measurements were made at 800 mm SAD.

## 2) Off-center ratio (OCR)

OCR is the ratio of the absorbed dose at a given off-axis

point relative to the dose at the radiation beam central axis (CAX) at the same depth. OCR data were taken for 11 fields. Measurement depths are 15, 50, 100, 200, and 300 mm. The OCRs were obtained from sets of orthogonal scans across the radiation field using fixed SSD method (800 mm) and 0.2 mm resolution for 20 mm or smaller field sizes and 0.5 mm resolution for field sizes greater than 20 mm. Then, the

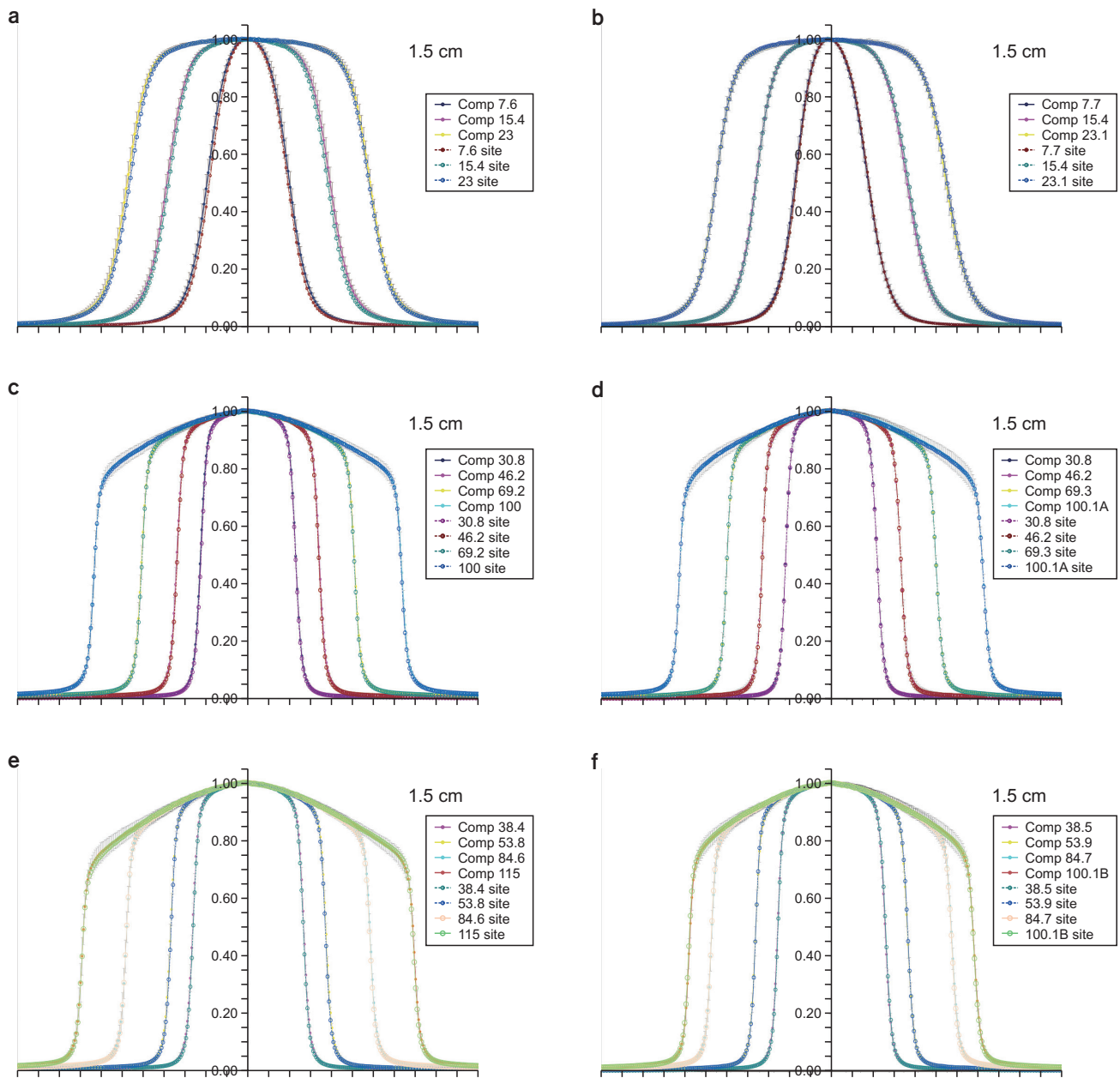


**Fig. 3.** Visual comparisons of OCRs between measurement and composite data at a depth of 15 mm. OCRs with (a) X field size of 7.6 mm, 15.4 mm, and 23 mm and (b) Y field size of 7.7 mm, 15.4 mm, and 23.1 mm. OCRs with (c) X field size of 30.8 mm, 46.2 mm, 69.2 mm, and 100 mm and (d) Y field size of 30.8 mm, 46.2 mm, 69.3 mm, and 100.1 mm. OCRs with (e) X field size of 38.4 mm, 53.8 mm, 84.6 mm, and 115 mm and (f) Y field size of 38.5 mm, 53.9 mm, 84.7 mm, and 100.1 mm.

measurements were geometrically converted as an SAD equivalent setup.

### 3) Output factor (OF)

OF is the ratio of the absorbed dose at a particular field size relative to the dose at a reference field. The reference field size for the Robotic IMRT is the 60 mm fixed collimator. By localizing a detector at a depth of 15 mm in the water phantom, OFs were measured at 800 mm SAD only. The measurements were normalized to 60 mm fixed collimator. We selected two detectors for small field measurements.

### 4) Open beam profiles

Four scans (0°, 45°, 90°, 135°) are required for open beam profiles. Measurements were performed at 800 mm SSD and the depth of 20 mm.

## 3. Validation of the model

The beam model created with these measurement data was verified by performing patient-specific QA in fiducial-inserted phantoms (Octavius 1000 SRS detector,<sup>6)</sup> stereotactic dose verification phantom, pelvis phantom, and thorax phantom), using 10 intracranial and extracranial patient plans.

## Results

All measurements for acceptance testing satisfied manu-

facture specifications. The result of EBT3 films analyzed using RIT software was shown in Fig. 1. Mean leaf position offsets using Garden Fence test were found to  $0.01 \pm 0.06$  mm and  $0.07 \pm 0.05$  mm for X1 and X2 leaf banks. All positions were less than 0.95 mm at 800 mm SAD deviation from expected positions. Each bank has no more than 13 leaf junctions higher than 0.5 mm (at 800 mm SAD) deviation from expected positions. Each leaf has no more than 1 position greater than 0.5 mm (at 800 mm SAD) deviation from expected positions. Fig. 2 shows the result of leakage film using ImageJ analysis. The maximum leakage of each film was 0.20% and average leakages of each film was 0.18%. E2E tests for five tracking modes showed that 0.26 mm (6D Skull), 0.3 mm (Fiducial), 0.26 mm (Xsight Spine), 0.62 mm (Xsight Lung), and 0.6 mm (Synchrony), respectively. E2E accuracy was less than 0.95 mm. All tests were successfully passed.

Table 1 shows the percent difference of TPR at various field size with PTW 60018 diode SRS detector. All

**Table 3.** Patient-specific QA results using Octavius 1000 SRS detector.

ID	Point dose error (%)	Gamma passing ratio (%)
p7514820	2.04	95.0
p2317947	3.87	92.7
p7863469	3.26	90.0
p8028173	0.62	97.6
p3863606	1.26	100.0
p7594455	-0.84	100.0
p8006687	0.46	97.7

**Table 2.** Percent differences of OFs between measurement and composite data.

X (mm)	Y (mm)	Composite data	PTW 60018 diode SRS (%)	PTW 60019 microDiamond (%)
7.6	7.7	0.818	-0.32	-1.53
15.4	15.4	0.950	-0.24	0.14
23.0	23.1	0.977	-0.22	0.14
30.8	30.8	0.987	-0.24	-0.03
38.4	38.5	0.993	-0.19	0.13
46.2	46.2	0.999	-0.17	0.05
53.8	53.9	1.003	-0.13	-0.35
69.2	69.3	1.011	-0.16	-0.21
84.6	84.7	1.017	-0.05	-0.35
100.0	100.1	1.022	-0.04	-0.29
115.0	100.1	1.023	0.08	-0.35



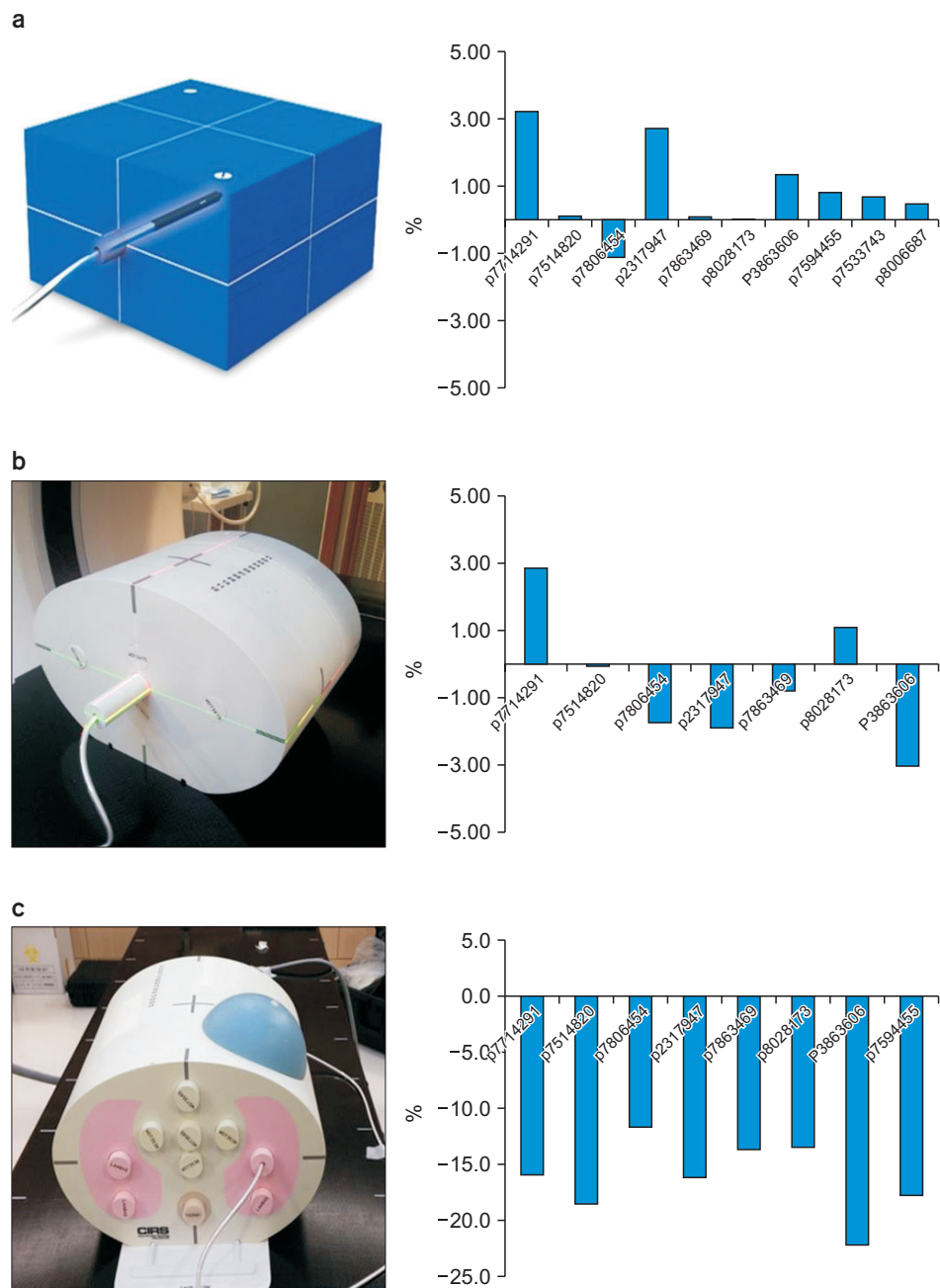


**Fig. 4.** Point dose errors of patient-specific QA: (a) stereotactic dose verification phantom, (b) pelvis phantom, and (c) thorax phantom.

measurements showed a good agreement within  $\pm 2\%$  except near-surface regions. Among 5 depths for OCR measurements, Fig. 3 shows OCRs between measurement and composite data at a depth of 15 mm for visual comparisons. They were in good agreement visually. Table 2 shows the percent difference of OFs between measurement and composite data. OFs measured by using two detectors agreed with composite data to within  $\pm 1.6\%$ . In particular, PTW 60018 diode SRS showed slightly better

correspondence in the smallest field such as 7.6 mm $\times$ 7.7 mm.

Patient-specific QA results using Octavius 1000 SRS detector were shown in Table 3. The point dose errors for each patient-specific QA were shown within  $\pm 5\%$ . The analysis was performed using 3%/3 mm gamma analysis criteria. The range of gamma passing ratio was from 90% to 100%. In Fig. 4, point dose errors of patient-specific QA could be shown within  $\pm 5\%$  except results of

**Table 4.** Patient-specific QA results using MC fixed cone for thorax phantom.

ID	Calculated dose (cGy)	Measured dose (cGy)	Difference (%)
p8028173	602.53	600.26	0.38
p8006687	511.57	512.12	-0.11
p7714291	598.43	587.62	1.84
p7594455	627.74	638.90	-1.75
p2317947	803.57	786.38	2.19

thorax phantom. The QA plans were calculated with FSPB algorithm. In heterogeneous region, the measurements of point dose were underestimated around 13~23%. To overcome this issue, Monte Carlo (MC) dose calculation algorithm<sup>5,7,8)</sup> should be considered with fixed cone. When MC was calculated in a medium resolution grid and with 2% statistical uncertainty, the percent differences of point dose were within  $\pm 3\%$  as shown in Table 4.

## Discussion

Acceptance testing and clinical dosimetry measurements have been presented here. Our measurements showed excellent agreement within 2% of the composite data, which are an average of the measurements made by several sites provided by the manufacturer.

If only InCise™2 MLC is added in a working Robotic IMRT M6 system, a total of 2 weeks should be enough, 1 week for acquisition and 1 week for treatment planning system (TPS) modelling and verification. According to the recent literature<sup>9)</sup> for beam data measurement, there have been several recommendations to apply  $K_Q$  value dependent on the field size and the dose-rate. Best case scenario is to use the W1 scintillator with corrections  $<0.5\%$  for all field sizes. The EDGE diode shows corrections within 1% (1000 mm SAD) and within 1.1% (650 mm SAD), but it is not included in the comparison at 800 mm SAD where it really matters for Robotic IMRT M6. Ion chambers require greater corrections (as high as 23%) dependent on both field size and orientation to the beam. Even the smallest microchambers are still too big. The pinpoint is long to be useful for the smallest field sizes. Even though pinpoint is only 2 mm thin, it is about 10 mm long. Considering volume, sensitivity, and the results discussed above, the

60018 diode SRS was used as beam data measurements.

As far as verifying the beam model, we performed multiple E2Es, did absolute dose verification for several plans (patient-specific QA including non-isocentric plans), and delivered single beam QA plans that were calculated in the TPS. By these verifications, we saw accurate robot alignment from the E2Es and also determined accurate dose calculation by the TPS in the simple single beam case as well as a full treatment.

For a mechanical QA to determine alignment between the MLC and the beam, a diode array such as SRS profiler (Sun Nuclear Corporation) can be considered as a daily QA because it shows the relationship between the beam peak and penumbra to show that the alignment has not changed. Picket fence is done daily to check field abutment; garden fence is done monthly to determine individual leaf position accuracy.

## Conclusion

Robotic IMRT M6 system equipped with InCise™2 MLC was proven to be accurate and reliable, and it is currently in clinical use.

## Acknowledgements

This research was supported by a grant of the Korea Health Technology R&D Project through the Korea Health Industry Development Institute (KHIDI) funded by the Ministry of Health & Welfare, Republic of Korea (HI16C0819), by a grant of the Radiation Technology R&D program through the National Research Foundation of Korea funded by the Ministry of Science, ICT & Future Planning (NRF-2017M2A2A6A01070330), and by a grant of the Basic Science Research Program through the National Research Foundation of Korea funded by the Ministry of Education (NRF-2015R1D1A1A01056850).

## Conflicts of Interest

The authors have nothing to disclose.

## Availability of Data and Materials

All relevant data are within the paper and its Supporting Information files.

## References

1. Eshleman JS, Berkenstock KG, Singapuri KP, Fuller C. The CyberKnife® M6™ radiosurgery system. *J Lanc Gen Hosp*. 2013;8: 44-49.
2. Kim N, Lee H, Kim JS, et al. Clinical outcomes of multileaf collimator-based CyberKnife for spine stereotactic body radiation therapy. *The British journal of radiology*. 2017;90: 20170523.
3. Barbotteau Y, Rignon A, Crespín M, et al. 22. CyberKnife M6 InCise-2 multileaf collimator setup, modelization and quality insurance program. *Physica Medica: European Journal of Medical Physics*. 2016;32: 351-352.
4. Kim J, Park K, Yoon J, et al. Feasibility Study of a Custom-made Film for End-to-End Quality Assurance Test of Robotic Intensity Modulated Radiation Therapy System. *Progress in Medical Physics*. 2016;27: 189-195.
5. Sudahar H, Kurup PG, Murali V, Velmurugan J. Influence of smoothing algorithms in Monte Carlo dose calculations of cyberknife treatment plans: A lung phantom study. *Journal of cancer research and therapeutics*. 2012;8: 367.
6. O'Connor P, Seshadri V, Charles P. Detecting MLC errors in stereotactic radiotherapy plans with a liquid filled ionization chamber array. *Australasian physical & engineering sciences in medicine*. 2016;39: 247-252.
7. Hoogeman MS, van de Water S, Levendag PC, van der Holt B, Heijmen BJ, Nuytens JJ. Clinical introduction of Monte Carlo treatment planning: a different prescription dose for non-small cell lung cancer according to tumor location and size. *Radiotherapy and Oncology*. 2010;96: 55-60.
8. Sharma S, Ott J, Williams J, Dickow D. Dose calculation accuracy of the Monte Carlo algorithm for CyberKnife compared with other commercially available dose calculation algorithms. *Medical Dosimetry*. 2011;36: 347-350.
9. Francescon P, Kilby W, Satariano N. Monte Carlo simulated correction factors for output factor measurement with the CyberKnife system—results for new detectors and correction factor dependence on measurement distance and detector orientation. *Physics in Medicine & Biology*. 2014;59: N11.